Arab J. Nucl. Sci. Appl., Vol. 56, 3, 81-94 (2023)

ISSN 1110-0451

Arab Journal of Nuclear Sciences and Applications

Web site: ajnsa.journals.ekb.eg

(E S N S A)

Evaluation of Radon Radioactivity and Radiological Impact by Using Solid-State Nuclear Track Detector for Erediya younger granites of Central Eastern Desert in Egypt

Fatma Qabeeli[1], Ahmed El-Khatib[1], Mahmoud Abass[1], Gehad Saleh[2], Mohamed Mitwalli[3,4]*

(1) Physics Department, Faculty of Science, Alexandria University, 21526 Alexandria, Egypt

(2) Nuclear Materials Authority, El-Maadi, P.O. Box 530, Cairo, Egypt

(3) Physics Department, Faculty of Science, Mansoura University, 35516 Mansoura, Egypt

(4) National Network for Nuclear Sciences, Academy of Scientific Research and Technology (NNS-ASRT), 11334 Cairo, Egypt

ARTICLE INFO

Article history:

Received: 5th Sept. 2022

Accepted: 5th Jan. 2023

Keywords:

Radium;
Nuclear Track Detector;
Environmental radioactivity;
Radiological hazards;
Erediya area.

ABSTRACT

The current study is carried out to monitor radioactivity levels in Erediya younger granites of the Central Eastern Desert in Egypt by using a solid-state nuclear track detector (CR-39 NTD). The polymeric CR-39 NTD was used to determine radium-226 and radon-222 activity concentration, and the theoretical conversion equations, were employed to assess the radiological impact. Predetermined 33 samples were collected from different locations within and around Egypt's Eradia area fulfilling the IAEA TECDOC-1415 protocols. The measured overall average value of the radium and radon activity concentration are 7467.44±50.68 and 7840.14±53.2 Bqm^{-3}, respectively, which indicated a high abundance of TENORM in the collected samples of the investigated area. The exhalation rate and annual effective dose were calculated, indicating high grades than the permissible limit recommended by IAEA and UNSCEAR, and the average values are 0.87±0.01 Bqm^{-2}h^{-1} and 1637.82±26.87 mSvy^{-1} respectively. The present result is a reference for the radioactivity background as well as assesses any harmful radiation, and particularly helps in applying radiation protection principles for the occupational worker in the Erediya area. To furnish the outcome of the study, data was plotted as counter maps for tracking the distribution pattern of radioactivity levels and concerning radiation protection and human safety work level index was calculated to apply perfect radiation protection methodologies for the occupational.

INTRODUCTION

Every day, public people and particularly operational and occupational inhale radionuclides from the air, soil, water, and food, since natural radioactivity is common in rocks and environmental soil, especially in uranium, coal, and mineral mines. The principal mechanisms of reaching radioactive isotopes are internal human body via inhalation of radon, thoron gases moreover the primordial radionuclides and their descendants [1]. ^{222}Rn is created as a noble gas by alpha-decay of ^{226}Ra in this series and is a part of the ^{222}Rn exhaled into the atmosphere by terrestrial and rocks. Radon is the most naturally occurring radioactive gas that is detrimental to the human population since it is one of the primary causes of skin and lung cancer [2, 3]. Uranium mineralization is structurally regulated and linked with jasperoid veins inside the Erediya granitic pluton in the Erediya area, Central Eastern Desert in Egypt. This granite has been altered extensively, with silicification, argillization, sericitization, chloritization, carbonatization, and hematization occurring [4-8].

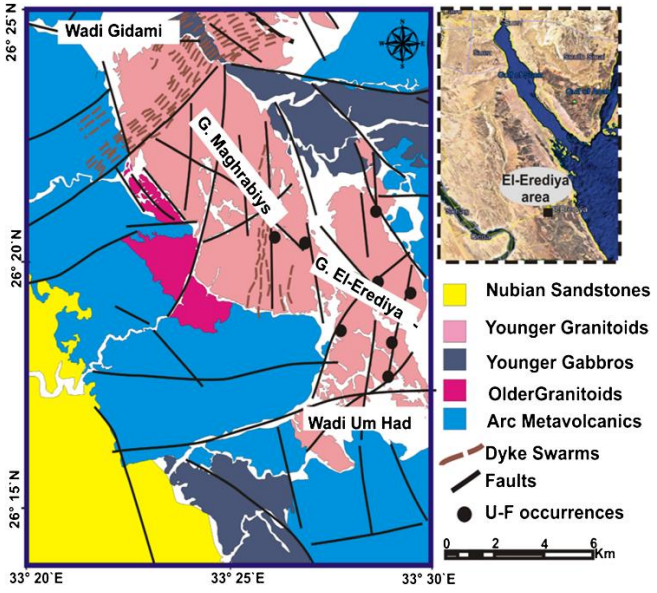

Fig. (1): The geological map of the Erediya area, Central Eastern Desert, Egypt, and the sample flow fields on the right side [9, 10]

Corresponding author: meto_mms@yahoo.com

DOI: 10.21608/ajnsa.2022.160908.1632

In addition to the previous studies concerning public health and environmental safety found that radon gas exposure increases the incidence of carcinogenic illnesses in the general population. Solid-State Nuclear Track Detectors (SSNTDs) are used widely in technical applications for numerous investigations of environmental radioactivity and geophysics studies. Environmental radiation is due to various radioactive nuclides present in the sediment and rocks distributed depending on the region's geological and geographical features, so radionuclides have been present on the earth's surface [11-15]. Among the different isotopes of radon, the study was carried to determine the concentration of ^{222}Rn, which decays with a half-life of 3.82 days into many short-lived but highly alpha emitter daughter progenies like ^{218}Po and ^{214}Po [16-20]. Radon with its daughter products is the highest contributor to human exposure to natural background radiation. Hence, it is considered an environmental and radio-biological health risk, particularly for enclosed areas such as underground mines, caves, and cellars otherwise inadequately ventilated and designed places. Therefore, the study is carried out to measure the radium-226 and radon-222 activity concentrations in addition to calculate the radiological impact on public health control and estimate the hazard of radiation exposure for occupational [11, 13, 14, 21, 22].

GEOLOGICAL SETTING

Gabal El-Erediya is an oval-shaped outline and elongated granite intrusion. It covers nearly 16 km^2. This locality also comprises several rock units that represent from oldest to youngest: metavolcanics, older granites, younger gabbros, and younger granites Fig. (1). The El-Erediya younger granites are dissected by two main faulting trends (NWSE and N-S), which play an important role in pathways for different hydrothermal or meteoric solutions, which cause different types of hydrothermal alterations [5, 23]. Uranium mineralization is associated with the hydrothermally altered parts of the Erediya granite and localized within several shears and fractured zones that are filled with jasperoid veins Fig. 3 (b). The area is highly altered, especially along the structural lines and around the shear zones, the most common alteration is silicification, sericitization, and kaolinization. The three types of alteration mainly occur in a consistent zonal arrangement in which silicification occurs in the innermost zone followed successively by sericitization and then by kaolinization. Widespread hematitization and manganese staining are superposed on these alterations [24].

MATERIALS AND ANALYSIS

Many previous studies concerning the geology of the Erediya mine area, [5, 7, 9, 25-27], are largely made of precambrian igneous and metamorphic bedrock that is unconformably overlain to the west by undeformed flat-lying igneous and metamorphic foundation. Nubian sandstone has a precambrian igneous and metamorphic substrate that is unconformably overlain to the west by undeformed flat-lying Nubian sandstone Fig. (1). Predetermined 33 samples were collected from different locations within and around Egypt's Eradia area as shown in Fig. (2).

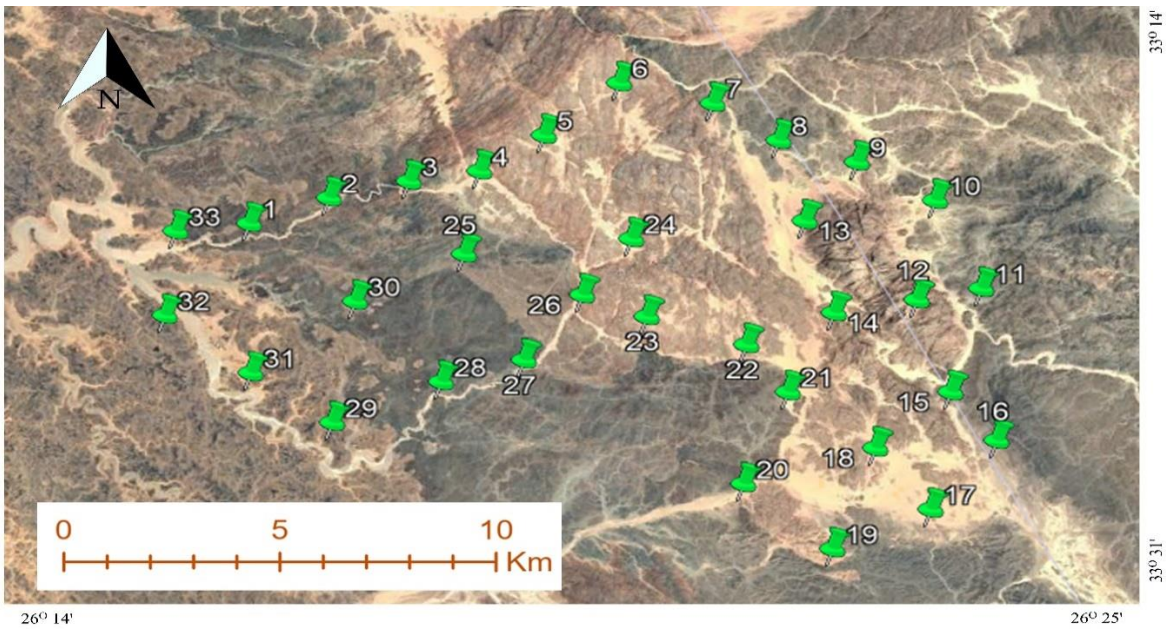

Fig. (2): The samples localities of El Erediya area, Central Eastern Desert, Egypt

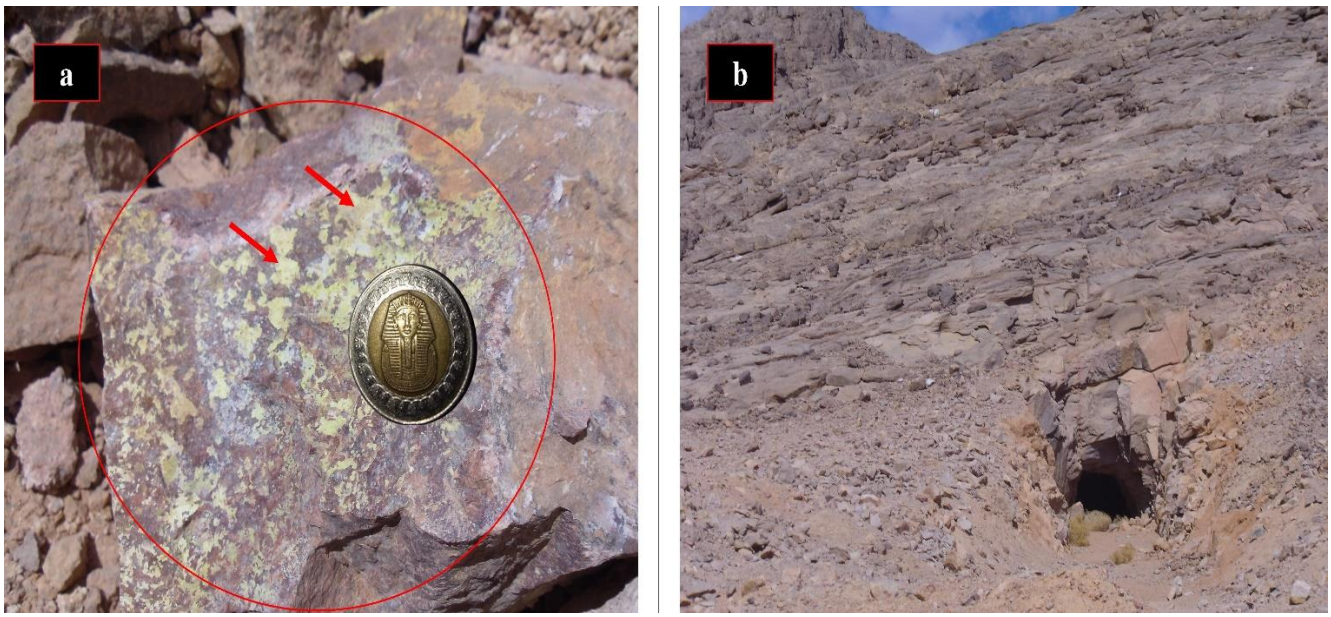

Fig. (3): View (a) sample of collected rocks significant with uranium mineralization limited by red cycle and View (b) Gabal El Erediya uriniferous shear zone (Photo by Gehad Saleh).

The methodology of collecting samples followed the recommendations protocol of IAEA [11]. The experimental investigation technique depended on the passive method to measure radium-226 and radon-222 activity concentrations. After the collecting process, the investigated samples were dried at 110°C for 60 minutes in the electric oven and sieved through a 1-mm to obtain a fine and homogenous powder of investigated samples. After accurate preparation, all samples were weighed and then sealed for 28 days in a closed cylindrical can made of stainless steel [13]. The Can's geometric dimension is 10.6 cm in diameter and 12 cm high, with a density of 7620 kgm^{-3}. The containers were capped tightly with an inverted cylindrical metal cover and about concerning standardization of the height of the samples inside the sealed can. The free distance between the surface of investigated samples and the installed polymer detectors was 8 cm. The CR-39 NTD, with 2 cm^2, was fixed at the bottom center of each inverted metal cover.

After the irradiation process mentioned above, which means that the decay of ^{226}Ra secular equilibrium has occurred, the CR-39 NTD were carefully removed from the cans cover. The CR-39 NTD were etched chemically via 6.25±0.05 N NaOH solution within 70±1°C for 8 hours, hence the CR-39 NTD were cleaned in distilled water and then immersed for 5 minutes in a 3% CH_3COOH solution with less than 1% water and over 98% concentration. Finally washed again with distilled water and dried in a closed plastic box [13, 28]. The tracks of alpha particles recorded on CR-39 NTD were counted using an optical microscope with a magnification of 640x. The experiment has taken care of the background of CR-39 NTD, which were calculated and subtracted from the total count of all samples [29-31]. The below-mentioned equations were employed for radiometric calculation and radioactivity monitoring as well radiological protection and assessment.

For calculating the concentration of radon (Bqm^{-3}) at secular equilibrium status, the following equation was used:

$$C_{Rn} = \frac{\rho}{\eta T} \pm \frac{\sqrt{\frac{\alpha}{f \pi r^2}}}{\eta T} \qquad (1)$$

where: C_{Rn} is radon concentration (Bqm^{-3}), ρ is the track density ($trackcm^{-2}$), T is the exposure duration (28 days), and η is the detector calibration factor of CR-39 [16].

$$\rho = \frac{\alpha}{f \pi r^2} \pm \sqrt{\frac{\alpha}{f \pi r^2}} \qquad (2)$$

where α is the summation of tracks, f is the number of investigated fields, πr^2 is the calibrated area of the

studied fields, T is the irradiation time (28 days), and η is the calibration coefficient of CR-39 detectors [13, 16, 32]

For calculating the levels of dissolved radon concenteation functional depth of investigated samples the following equation was used [33, 34]:

$$Cs_{Rn} = \frac{d\ t\ \lambda_{Rn}\ C_{Rn}}{h} \qquad \textbf{(3)}$$

where Cs_{Rn} is the dissolved radon concentration, d is the free distance between the surface of sample and CR-39 NTD (m), t is the exposure time (h), λ is the radon decay constant h^{-1}, C_{Rn} is the radon concentration measured with CR-39 NTD in Bqm^{-3} and h is the height of stored sample in (m).

For calculating the radon surface exhalation rate, the following equation was used:

$$E_A = \frac{C_{Rn}\ V\ \lambda}{A\ T_e} \pm \frac{\sqrt{\frac{\alpha}{f\pi r^2}}\ V\ \lambda}{\eta T A\ T_e} \qquad \textbf{(4)}$$

$$E_M = \frac{C_{Rn}\ V\ \lambda}{M\ T_e} \pm \frac{\sqrt{\frac{\alpha}{f\pi r^2}}\ V\ \lambda}{\eta T M\ T_e} \qquad \textbf{(5)}$$

$$T_e = [T + \frac{1}{\lambda}(e^{-\lambda T} - 1)] \qquad \textbf{(6)}$$

where E_A is exhalation rate ($Bqm^{-2}h^{-1}$), E_M is exhalation rate ($Bqkg^{-1}h^{-1}$), λ radon decay constant (0.00756 h^{-1}), C_{Rn} radon concentration (Bqm^{-3}), V is the volume of the closed Can (m^3), A is the surface area covered by sample (m^2), M is the mass of the sample (kg), T is the irradiation time [16, 35] and T_e is effective time which is related to the actual exposure time *T* and decay constant λ for ^{222}Rn [16, 36, 37].

The following equation was used to estimate the annual effective dose D_E:

$$D_E = A\ H\ F\ T\ C_{Rn} \pm \frac{A\ H\ F\ T\sqrt{\frac{\alpha}{f\pi r^2}}}{\eta T} \qquad \textbf{(7)}$$

where D_E is the annual effective dose, A is the conversion coefficient (9×10^{-6} $mSvh^{-1}$ / Bqm^{-3}), H is the indoor occupancy factor (0.8), F=0.4 is the indoor equilibrium factor between radon and its progeny, and T is the indoor exposure time in hours per year which, equal 2000 hy^{-1} [14, 38].

The working levels were calculated by using the following equation [39]:

$$WL = \frac{C_{Rn}\ x\ f}{3700} \pm \frac{\sqrt{\frac{\alpha}{f\pi r^2}}\ x\ f}{\eta T\ x\ 3700} \qquad \textbf{(8)}$$

where C_{Rn} is radon concentration in Bqm^{-3}, f is the equilibrium factor for radon has been taken as 0.4 by ICRP [14, 18, 20, 21, 40], and 3700 is the conversion factor to Working levels [14, 18, 41].

The effective radium content ($Bqkg^{-1}$) was calculated by the following equation:

$$C_{Ra} = \frac{\alpha h A}{M f \pi r^2\ T_e} \pm \frac{h A\sqrt{\frac{\alpha}{f\pi r^2}}}{M\ T_e} \qquad \textbf{(9)}$$

where C_{Ra} is the effective radium content of investgated samples ($Bqkg^{-1}$), *M* is the mass of sample (kg), *A* is the area of cross-section of the container (0.01 m^2), *h* is the distance between the detector and the top of the sample (0.08 m), *f* is the sensitivity factor to (0.18 $tracks\cdot cm^{-2}\cdot d^{-1}/Bqm^{-3}$) and T_e is the effective exposure time.

The alpha radiation index from the radon inhalation and originating from the exploration and geological process was calculated by tht following equation [42]:

$$I\alpha = \frac{C_{Ra}}{200} \qquad \textbf{(10)}$$

where Iα is the alpha radiation index, C_{Ra} is the effective radium content of investigated samples ($Bqkg^{-1}$), and 200 is the conversion coefficient.

RESULTS AND DISCUSSION

Table (2) shows the values of track density, radon concentration, dissolved radon concentration, surface

exhalation rate, and mass exhalation rate of the investigated samples using CR-39 NTD. The values of track density are ranged from 6323 to 177544 Trackcm^{-2} with an average value of 70561.27 Trackcm^{-2}. The radon concentrations are ranged from 702.56±3.11 to 19727.11±125.78 Bqm^{-3} with an average value of 7840.14±53.24 Bqm^{-3}. The radon concentration is different from one sample to another due to the variation in the chemical composition and geological structure of the samples as a function of uranium immigration strategy moreover rocks bearing heavy elements, especially uranium mineralization as shown in Fig. 3 (a) where the related work concerning the chemical composition find the uranium-bearing minerals in Erediya area with the majority of the uranium minerals are pyrochlore group [43] as well the pyrochlore group's known U-rich (U>0.4 atom per formula unit) species include uranpyrochlore, uranmicrolite, and betafite. REE, U, and Th are often found in pyrochlore group minerals. Because of this property, this structure type is one of the primary actinide host phases for nuclear waste disposal, and it is one of the ingredients of Synroc [44-46].The radon concentration values are higher than the permissible and recommended limit of 1000 Bqm^{-3} [14, 18-20, 41, 47]. Based on the radon concentration the dissolved concentrations of radon are ranged from 301.15±1.33 to 8351.67±53.25 Bqm^{-1} with an average value of 2074.03±15.83 Bqm^{-1}. The surface exhalation rate is ranged from 8.39±0.49 to 237.35±2.96 Bqm^{-2}h^{-1} with an average value of 94.077±1.52 Bqm^{-2}h^{-1}. Because of the variety of samples density, the mass exhalation rate is calculated and ranged from 6.59±0.03 to 186.41±1.19 Bqkg^{-1}h^{-1} with an average of 73.88±0.5. Table (2) shows the values of radon concentration, radium activity concentration, alpha index, annual effective dose, and work level values. The activity concentration is calculated to monitor the radioactivity levels of investigated samples which help to record the background of radiation in the area under study. The values of radium-226 are ranged from 714.01±3.16 to 7467.44±50.68 Bqm^{-3} with an average value of 18966.01±120.93. Concerning radiological impact estimation the alpha index is calculated and ranged from 3.29±0.01 to 93.2±0.59 with an average value of 36.94±0.25 as well as the annual effective dose varied from 47.8±1.02 to 13592.7±115.02 mSvy^{-1} with an average of 1637.82±26.87 mSvy^{-1}, which is higher than the permitted dose of 20 mSvy^{-1} recommended by [40, 48]. The dose level of annual effectiveness is more elevated than the recommended level [40]. The worldwide average value is equal to 1 mSvy^{-1} and corresponds to the annual effective dose equivalent of 1 mSvy^{-1} for the public [14]. The permissible dose of occupational radiation exposure is 20 mSvy^{-1} in all European countries and 50 mSvy^{-1} in the USA. The obtained results compatible with the literature work for similar environments [13, 18, 29, 49-54] in addition Table (3) present the recorded measurements in different countries. Fig. (4) shows a comparison of radon concentration results for CR-39 NTD. Sample No. (10), with the code (ED10), exhibits a high radon content. That is, the radon concentration values are high in this position due to an increase in the level of ^{238}U and ^{226}Ra activity concentration; however, sample No. (28), its cod (T207), indicated the lowest value of radon concentration, and frequencies of radon concentration range of investigated samples are included in the top part of the figure.

The correlation between radon concentration and its dissolves measured by CR-39 NTD is shown in Fig. (5), with R^2 = 0.99, significant a high agreement between radon concentration measurement and surface exhalation rate as presented in figures (6) in addition to significant correlation relation between radium and radon concentration measured by CR-39 NTD as shown in Fig. (7) and Fig (8) which conducted to correlation between (radon concentration and its surface exhalation rate), (radon concentration and its mass exhalation rate), and its ration that indicate significant measurements of radon in the secular equilibrium phase For monitoring the radioactivity levels for the Erediya area the activity concentration of radium-226 was tracked by contour maps as shown in Fig. (9).

Table (1): The values of track density, radon concentration, dissolved radon concentration, surface exhalation rate, and mass exhalation rate

NO	Code	ρ Trackcm^{-2}	C_{Rn-222} Bqm^{-3}	Cs_{Rn-222} Bqm^{-3}	E_A Bqm^{-2}h^{-1}	E_M Bqkg^{-1}h^{-1}
1	ED1	23809±415	2645.44±46.11	1147.97±20.01	31.83±1.69	24.93±0.43
2	ED2	34483±499	3831.44±55.44	1723.46±24.94	46.1±0.64	35.69±0.52
3	ED3	50580±604	5620±67.11	2230.58±26.64	67.62±1.05	54.35±0.65
4	ED4	103781±865	11531.22±96.11	4942.88±41.2	138.74±0.57	113.84±0.95
5	ED5	97366±838	10818.44±93.11	4408.34±37.94	130.16±2.96	99.11±0.85
6	ED6	62692±673	6965.78±74.78	3096.48±33.24	83.81±2.46	64.9±0.7
7	ED7	108930±887	12103.33±98.56	5316.22±43.29	145.62±0.81	115.36±0.94
8	ED8	108469±885	12052.11±98.33	5102.38±41.63	145.01±1.39	117.58±0.96
9	ED9	137515±996	15279.44±110.67	6549.56±47.44	183.84±2.94	148.19±1.07
10	ED10	177544±1132	19727.11±125.78	8351.67±53.25	237.35±1.02	189.66±1.21
11	ED11	160164±1075	17796±119.44	7345.76±49.3	214.12±2.27	176.22±1.18
12	ED12	149233±1038	16581.44±115.33	7107.67±49.44	199.5±1.26	157.58±1.1
13	ED13	17041±351	1893.44±39	761.53±15.69	22.78±1.59	17.74±0.37
14	ED14	25329±428	2814.33±47.56	1102.12±18.62	33.86±1.16	25.93±0.44
15	ED15	37826±523	4202.89±58.11	1912.79±26.45	50.57±1.09	37.88±0.52
16	ED16	79130±756	8792.22±84	3815.33±36.45	105.79±0.72	79.89±0.76
17	ED17	74149±732	8238.78±81.33	3095.57±30.56	99.13±0.49	79.67±0.79
18	ED18	47229±584	5247.67±64.89	2277.19±28.16	63.14±1.29	46.04±0.57
19	ED19	83127±775	9236.33±86.11	4154.69±38.73	111.13±2.05	92.85±0.87
20	ED20	82769±773	9196.56±85.89	3796.12±35.45	110.65±1.64	87.65±0.82
21	T200	12815±106	1423.89±11.78	595.28±4.92	17.12±1.63	13.72±0.11
22	T201	21514±100	2390.44±11.11	1024.67±4.76	28.71±1.63	22.61±0.11
23	T202	13247±65	1471.89±7.22	576.4±2.83	17.66±1.63	14.24±0.07
24	T203	15899±62	1766.56±6.89	710.49±2.77	21.18±1.63	16.87±0.07
25	T204	11579±47	1286.56±5.22	503.83±2.04	15.41±1.63	11.54±0.05
26	T205	9047±38	1005.22±4.22	425.57±1.79	12.03±1.63	9.69±0.04
27	T206	7662±33	851.33±3.67	364.93±1.57	10.18±1.63	7.88±0.03
28	T207	6323±28	702.56±3.11	301.15±1.33	8.39±1.62	7.14±0.03
29	T208	78088±92	8676.44±10.22	3260.02±3.84	103.52±1.62	84.44±0.1
30	T209	117514±108	13057.11±12	5044.17±4.64	155.64±1.62	122.94±0.11
31	T210	106535±98	11837.22±10.89	4823.48±4.44	140.97±1.62	111.03±0.1
32	T211	122486±100	13609.56±11.11	5761.74±4.7	161.93±1.62	121.28±0.1
33	T212	144647±105	16071.89±11.67	7144.4±5.19	191.05±1.62	155.83±0.11
Ava.		70561.27	7840.14±53.24	2074.03±15.83	94.077±1.52	73.88±0.5
Max.		177544	19727.11±125.78	8351.67±53.25	237.35±2.96	186.41±1.19
Min.		6323	702.56±3.11	301.15±1.33	8.39±0.49	6.59±0.03
S.D.		51491.66	5721.29±41.68	2427.23±17.75	68.62±0.58	53.89±0.39

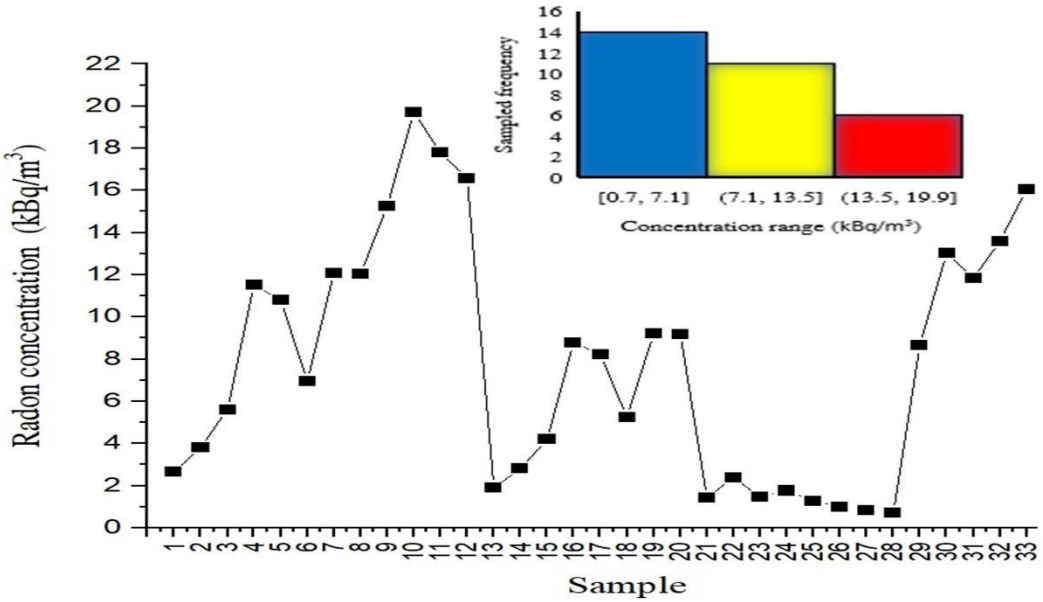

Fig. (4): Comparison between radon concentration recorded by CR-39 NTD.

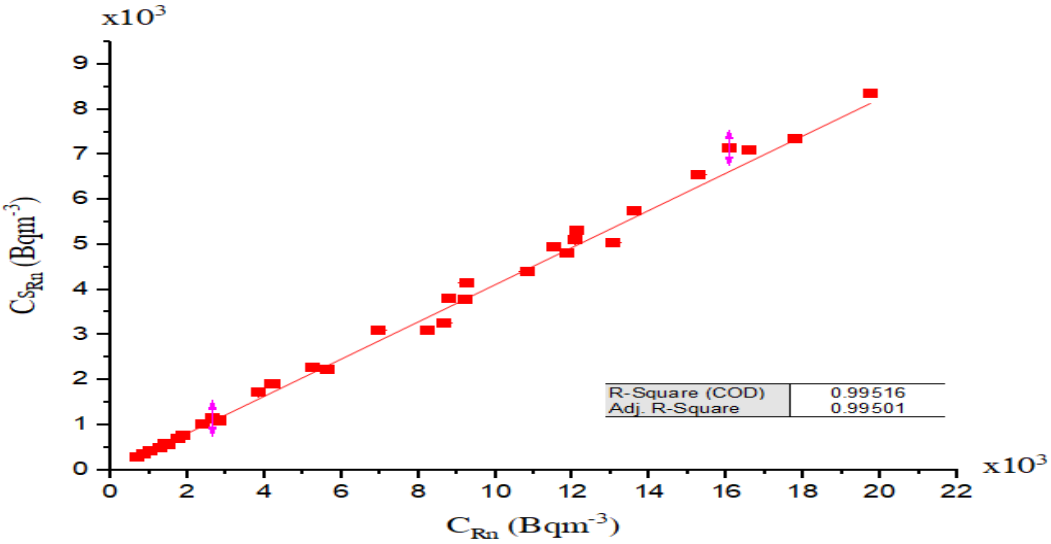

Fig. (5): Correlation relation between radon concentration and its dissolution measured by CR-39.

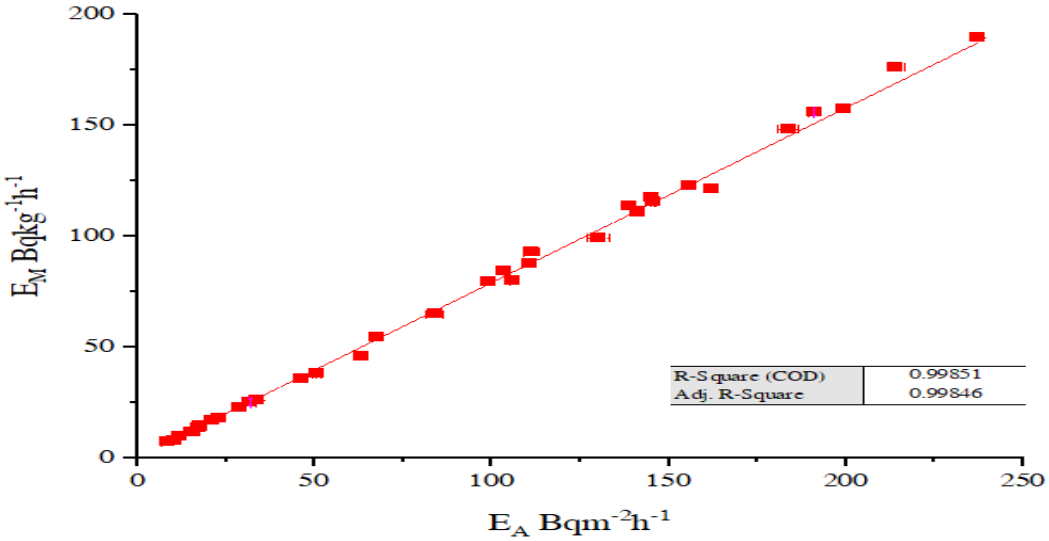

Fig. (6): Correlation relation between radon surface exhalation rate, and mass exhalation rate measured by CR-39 NTD.

Table (2): The values of radon concentration, radium activity concentration, alpha index, annual effective dose, and work level values

NO	Code	C_{Rn} Bqm^{-3}	C_{Ra} Bqm^{-3}	Alpha index	D_E $mSvy^{-1}$	WL Bqm^{-3}
1	ED1	2645.44±46.11	2492.66±43.45	12.5±0.22	66.79±3.55	0.29±0.02
2	ED2	3831.44±55.44	3569.48±51.65	18.1±0.26	96.73±1.34	0.41±0.01
3	ED3	5620±67.11	5434.77±64.9	26.55±0.32	141.88±2.2	0.61±0.01
4	ED4	11531.22±96.11	11384.17±94.89	54.48±0.45	291.12±1.19	1.25±0.01
5	ED5	10818.44±93.11	9911.25±85.3	51.11±0.44	273.12±6.21	1.17±0.03
6	ED6	6965.78±74.78	6489.51±69.67	32.91±0.35	175.86±5.17	0.75±0.02
7	ED7	12103.33±98.56	11535.76±93.93	57.18±0.47	305.56±1.71	1.31±0.01
8	ED8	12052.11±98.33	11758.02±95.93	56.94±0.46	304.27±2.92	1.3±0.01
9	ED9	15279.44±110.67	14819.17±107.33	72.19±0.52	385.75±6.17	1.65±0.03
10	ED10	19727.11±125.78	18966.01±120.93	93.2±0.59	498.03±2.14	2.13±0.01
11	ED11	17796±119.44	17621.66±118.27	84.08±0.56	449.28±4.77	1.92±0.02
12	ED12	16581.44±115.33	15758.47±109.61	78.34±0.54	418.62±2.65	1.79±0.01
13	ED13	1893.44±39	1773.98±36.54	8.95±0.18	47.8±3.34	0.2±0.01
14	ED14	2814.33±47.56	2592.7±43.81	13.3±0.22	71.05±2.44	0.3±0.01
15	ED15	4202.89±58.11	3787.5±52.37	19.86±0.27	106.11±2.29	0.45±0.01
16	ED16	8792.22±84	7988.55±76.32	41.54±0.4	221.97±1.5	0.95±0.01
17	ED17	8238.78±81.33	7967.23±78.65	38.93±0.38	208±1.02	0.89
18	ED18	5247.67±64.89	4603.58±56.92	24.79±0.31	132.48±2.7	0.57±0.01
19	ED19	9236.33±86.11	9284.84±86.56	43.64±0.41	233.18±4.31	1±0.02
20	ED20	9196.56±85.89	8765.3±81.86	43.45±0.41	232.18±3.43	0.99±0.01
21	T200	1423.89±11.78	1371.66±11.35	6.72±0.06	125.82±12.02	0.15±0.01
22	T201	2390.44±11.11	2261.06±10.51	11.27±0.05	362.1±20.6	0.26±0.01
23	T202	1471.89±7.22	1423.55±6.99	6.93±0.03	315.86±29.18	0.16±0.01
24	T203	1766.56±6.89	1687.16±6.58	8.32±0.03	490.58±37.77	0.19±0.01
25	T204	1286.56±5.22	1154±4.68	6.05±0.02	438.49±46.35	0.14±0.01
26	T205	1005.22±4.22	969.49±4.07	4.72±0.02	406.05±54.94	0.11±0.01
27	T206	851.33±3.67	787.96±3.39	4±0.02	397.62±63.52	0.09±0.01
28	T207	702.56±3.11	714.01±3.16	3.29±0.01	372.47±72.1	0.08±0.01
29	T208	8676.44±10.22	8443.79±9.95	40.65±0.05	5147.59±80.69	0.94±0.01
30	T209	13057.11±12	12293.91±11.3	61.12±0.06	8570.66±89.27	1.41±0.01
31	T210	11837.22±10.89	11103.09±10.21	55.36±0.05	8517.04±97.85	1.28±0.01
32	T211	13609.56±11.11	12128.16±9.9	63.59±0.05	10651.23±106.44	1.47±0.01
33	T212	16071.89±11.67	15583.04±11.31	75.02±0.05	13592.7±115.02	1.74±0.01
Ava.		7840.14±53.24	7467.44±50.68	36.94±0.25	1637.82±26.87	0.85±0.01
Max.		19727.11±125.78	18966.01±120.93	93.2±0.59	13592.7±115.02	2.13±0.01
Min.		702.56±3.11	714.01±3.16	3.29±0.01	47.8±1.02	0.08
S.D.		5721.29±41.68	5518.19±40.208	26.94±0.20	3467.46±36.34	0.62±0.01

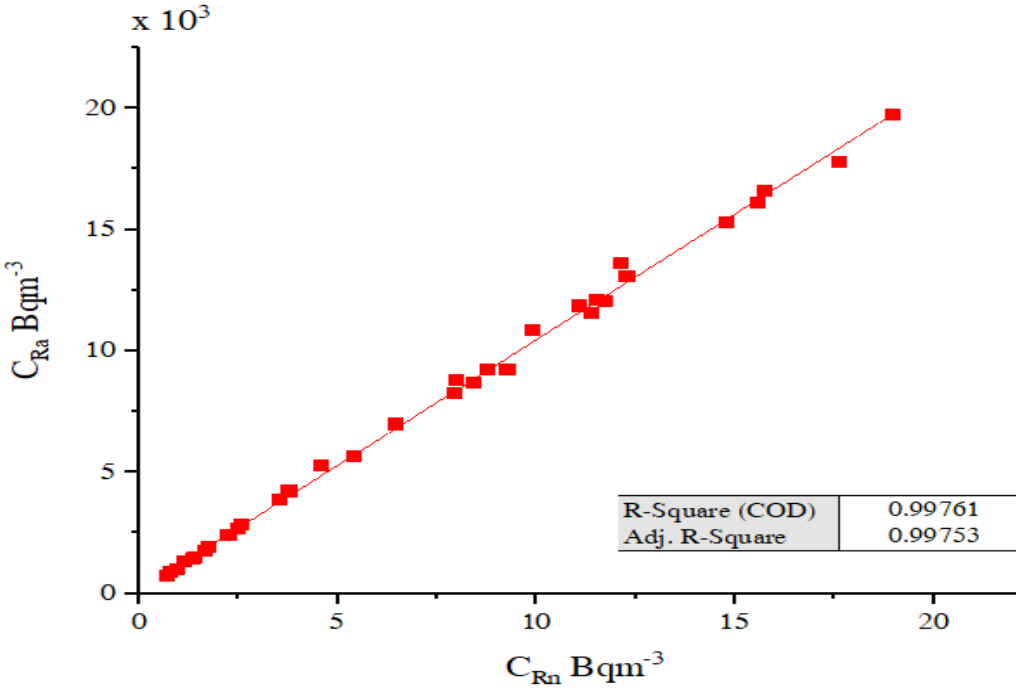

Fig. (7): Correlation relation between radium and radon concentration measured by CR-39.

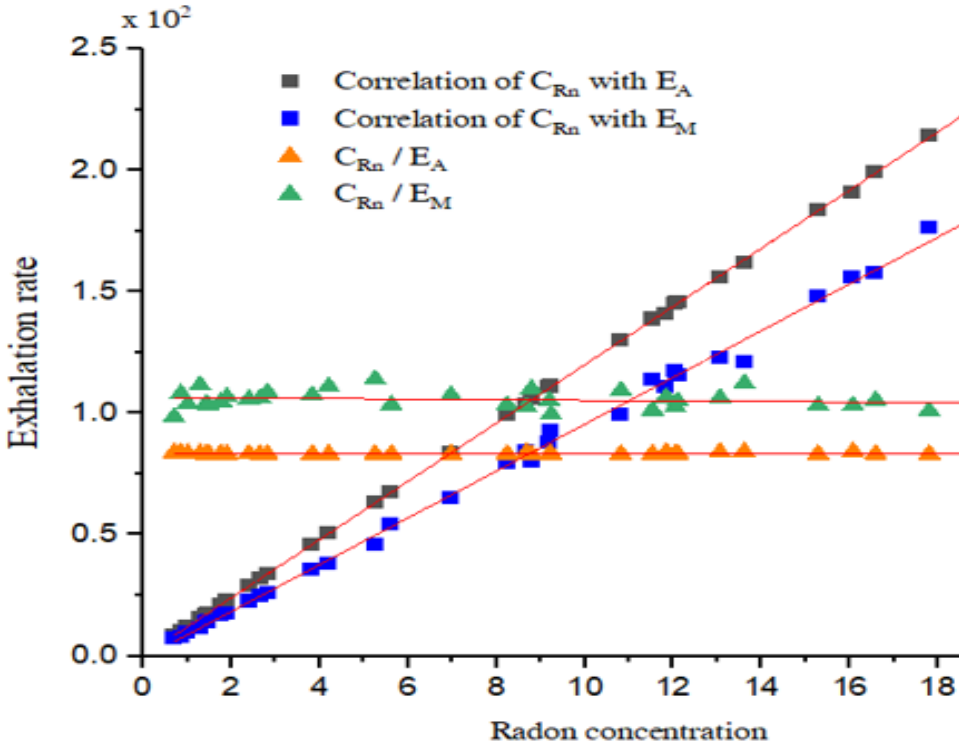

Fig. (8): Correlation relation between (radon concentration and surface exhalation rate), and (radon concentration and mass exhalation rate), measured by CR-39 NTD.

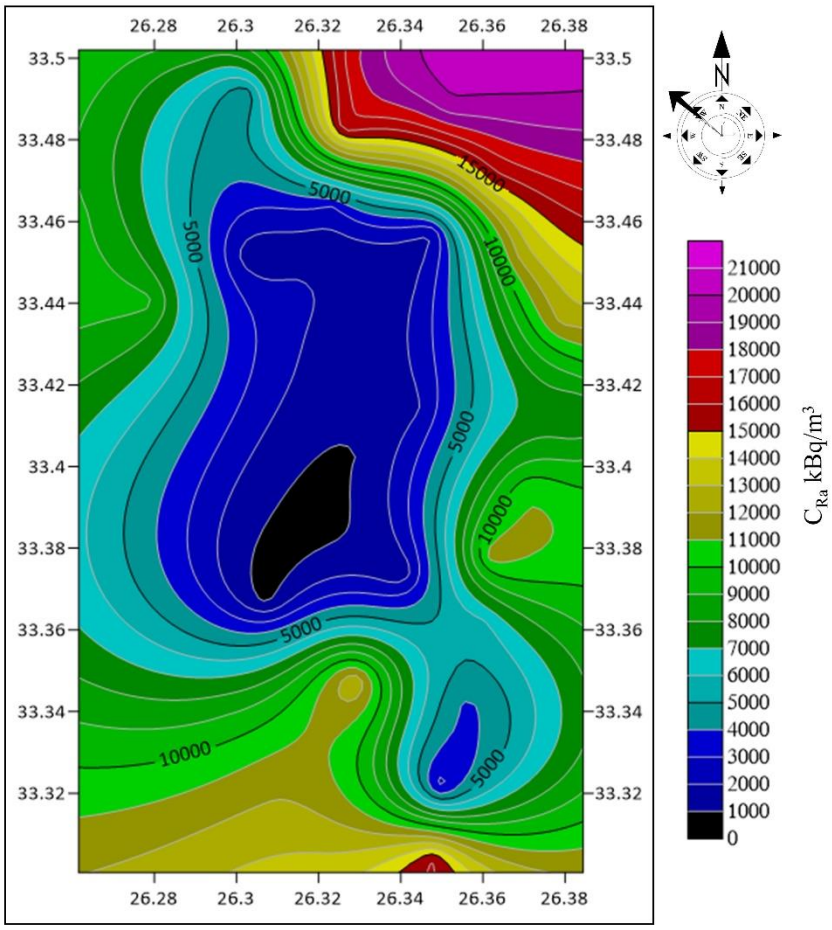

Fig. (9): Contour map for tracking the distribution pattern of Radium concentration for the Erediya area, Central Eastern Desert, Egypt.

Table (3): The recorded measurements for radioactivity level in different countries

Country	Area/Category	C_{Ra} (Bqm^{-3})	C_{Rn} (Bqm^{-3})	E_A (Bqm^{-2}h^{-1})	Reference
Egypt	Abu Rusheid	na	5121.05	1.83	[55]
Egypt	Al-Qusair	322.95	98.82	15.56	[28]
Egypt	Granite	32.46	136.19	88.02	[56]
Egypt	(Safaga)	32.00	20045.3	18.07	[57]
Egypt	Rocks	na	29,000	26.24	[35]
Egypt	Phosphat ore	22.18	1675.40	4.12	[34]
India	Soil	na	277.78	0.348	[58]
Cameron	Fertilizers	na	653.82	n/a	[59]
Pakistan	Uranium ore	na	7891	n/a	[60]
Egypt	Granites	7467.44±50.68	7840.14±53.24	94.077±1.52	Present work

CONCLUSIONS

The present work is organized and carried out for environmental radioactivity measurements. Ecological processes are very complex and unpredictable. Remarkably, the migration of pollutants (radionuclides) in sediments is hard to follow. Therefore, systematic studies are needed. The story presented in the manuscript was prepared systematically, and what is essential is that the estimates are described with uncertainty analysis. This aspect gives higher credibility to the results of the research. Geological materials are usually contaminated with TE-NORM. The current research reveals that the Eradia area is heavily polluted with radon concentration; hence, study findings aid in determining the places in the Eradia area with the greatest and lowest radon concentration values. In addition, the fluctuation of the concentration of the radioactive radionuclides that impact the environment may be detected. The average concentrations of radon levels are higher than the limitation (1000 Bqm^{-3}), recommended by (ICRP) [40], and it is generally higher than the reference level in workplaces, which (1500 Bqm^{-3}), which is recommended by (UNSCEAR and IAEA) [19, 21]. The data analysis records the radioactivity background levels in rock samples and is used as a reference to identify any change in the radioactive background level caused by geological processes.

STATEMENTS AND DECLARATIONS

The authors declare that they do not have any known competing financial interests or personal relationships that could appear to have influenced the current research paper. The authors declare that no clinical trials were conducted in the present study.

DATA AVAILABILITY STATEMENTS

All radiometric data and analysis of investigated samples are included in the current research paper.

REFERENCES

[1] Misdaq, M. and A. Mortassim, *222RN and 220RN concentrations measured in various natural honey samples by using nuclear track detectors and resulting radiation doses to the members of the rural populations in Morocco.* Radiation protection dosimetry, 2008. **130**(1): p. 115-118.

[2] Przylibski, T.A., *Radon and its daughter products behaviour in the air of an underground tourist route in the former arsenic and gold mine in Złoty Stok (Sudety Mountains, SW Poland).* Journal of Environmental Radioactivity, 2001. **57**(2): p. 87-103.

[3] Przylibski, T.A., *Concentration of 226Ra in rocks of the southern part of Lower Silesia (SW Poland).* Journal of Environmental Radioactivity, 2004. **75**(2): p. 171-191.

[4] Attawiya, M., *Mineralogical study of El-ERADYA-1, uranium occurrence, Eastern Desert, Egypt.* Arab Journal of Nuclear Sciences and Applications, 1983. **16**(2): p. 221-235.

[5] Hussein, H., M. El Tahir, and A. Abu-Deif. *Uranium mineralization through exploratory mining work, south Qena-Safaga midway, Eastern Desert, Egypt*. in *3rd Mining, Petroleum and Metallurgy Conference. Egypt, Cairo University*. 1992.

[6] Gangolly, J.S., et al., *Harmonization of the auditor's report.* The international journal of accounting, 2002. **37**(3): p. 327-346.

[7] Baldrian-Hussein, F., *Lü Tung-pin in Northern Sung Literature.* Cahiers d'Extrême-Asie, 1986(2): p. 133-169.

[8] Kröner, A., et al., *Dating of late Proterozoic ophiolites in Egypt and the Sudan using the single grain zircon evaporation technique.* Precambrian Research, 1992. **59**(1-2): p. 15-32.

[9] BAKHIT, F.S. and I.A.E. Kassas, *Distribution and orientation of radioactive veins in the El Erediya-El Missikat area, Central Eastern Desert, Egypt.* International Journal of Remote Sensing, 1989. **10**(3): p. 565-581.

[10] Abu Dief, A., *The relation between the uranium mineralization and tectonics in some Pan-African granite, west of Safaga, Eastern Desert, Egypt.* (PhD Thesis). Assuit University, 1993.

[11] IAEA, *Radiation Protection against Radon in Workplaces other than Mines*. 2004, Vienna: INTERNATIONAL ATOMIC ENERGY AGENCY.

[12] Ongori, J.N., et al., *Determining the radon exhalation rate from a gold mine tailings dump by measuring the gamma radiation.* J Environ Radioact, 2015. **140**: p. 16-24.

[13] Saleh, G.M., et al., *Environmental Radioactivity of Radon and its Hazards in Hamash Gold Mine, Egypt.* Arab Journal of Nuclear Sciences and Applications, 2019. **52**(4): p. 190-196.

[14] UNSCEAR, *Sources and Effects of Ionizing Radiation,* ed. R.t.t.G. Assembly. Vol. 1. 2000, New York: United Nations Scientific Committee on the Effects of Atomic Radiation.

[15] Mitwalli, M., et al., *Environmental Radioactivity Monitoring Using High Resolution Gamma-ray Spectrometer for Lake Manzala in Egypt.* Arab Journal of Nuclear Sciences and Applications, 2022. **55**(4): p. 139-149.

[16] Abbas, Y.M., et al., *Measurement of 226Ra concentration and radon exhalation rate in rock samples from Al-Qusair area using CR-39.* Journal of Radiation Research and Applied Sciences, 2020. **13**(1): p. 102-110.

[17] Ahmad, N., M.S. Jaafar, and S.A. Khan, *Correlation of radon exhalation rate with grain size of soil collected from Kedah, Malaysia.* Sci. Int, Lahore, 2014. **26**(2): p. 691-696.

[18] IAEA, *Analytical Methodology for the Determination of Radium Isotopes in Environmental Samples*. 2011, Vienna: International Atomic Energy Agency.

[19] IAEA, *Nuclear Data for the Production of Therapeutic Radionuclides*. 2012, Vienna: International Atomic Energy Agency.

[20] ICRP, *Protection Against Radon-222 at Home and at Work.* 1993, ICRP. p. . Ann. ICRP 23 (2).

[21] UNSCEAR, *Report of the United Nations Scientific Committee on the Effects of Atomic Radiation* UNSCEAR, 2011. **58**: p. 12.

[22] Zhuo, W., et al., *Estimating the amount and distribution of radon flux density from the soil surface in China.* J Environ Radioact, 2008. **99**(7): p. 1143-8.

[23] Abd El-Naby, H.H. and Y.H. Dawood, *Natural attenuation of uranium and formation of autunite at the expense of apatite within an oxidizing environment, south Eastern Desert of Egypt.* Applied Geochemistry, 2008. **23**(12): p. 3741-3755.

[24] Saleh, G.M., *Uranium Mineralization in Shear Zones: An Overview.* International. J. Min. Sci, 2020. **6**(1): p. 1.

[25] Ageel, A., K. El-Tahir, and A. Abu-Jayyb, *Effect of bromocriptine on prostacyclin release and cyclic nucleotides on rat aortic and uterine tissues.* Prostaglandins, 1985. **30**(3): p. 369-381.

[26] Abu-Deif, A., H. Abouelnaga, and H. Hassanein, *Distribution of radioelements and its relation to uranium migration, El Erediya exploratory tunnels, central Eastern Desert, Egypt.* J King Abdulaziz Univ (Earth Sci), 2001. **13**: p. 19-40.

[27] El-Naby, A. and H. Hamdy, *Genesis of secondary uranium minerals associated with jasperoid veins, El Erediya area, Eastern Desert, Egypt.* Mineralium Deposita, 2008. **43**(8): p. 933-944.

[28] Abbas, Y., et al., *Measurement of 226Ra concentration and radon exhalation rate in rock samples from Al-Qusair area using CR-39.* Journal of radiation research and applied sciences, 2020. **13**(1): p. 102-110.

[29] Singh, S. and S. Prasher, *The etching and structural studies of gamma irradiated induced effects in CR-39 plastic track recorder.* Nuclear Instruments and Methods in Physics Research Section B: Beam Interactions with Materials and Atoms, 2004. **222**(3): p. 518-524.

[30] Green, P.F., et al., *A study of bulk-etch rates and track-etch rates in CR39.* Nuclear Instruments and Methods in Physics Research, 1982. **203**(1): p. 551-559.

[31] El Ghazaly, M. and N.M. Hassan, *Characterization of saturation of CR-39 detector at high alpha-particle fluence.* Nuclear Engineering and Technology, 2018. **50**(3): p. 432-438.

[32] MITWALLI, M., et al., *Radon Measurement and Radiological Dose Assessment From Terrestrial Rocks Using Solid-State Nuclear Track Detectors.* Arab Journal of Nuclear Sciences and Applications, 2022: p. 1-8.

[33] Challan, M.B. and A.A. Labib, *Radiological assessment of exposure doses and radon exhalation rates of building materials in Saudi Arabia.* J Radiol Oncol, 2018. **2**: p. 012-021.

[34] Saad, A., *Radium activity and radon exhalation rates from phosphate ores using CR-39 on-line with an electronic radon gas analyzer "Alpha GUARD".* Radiation measurements, 2008. **43**: p. S463-S466.

[35] Abd-Elzaher, M., *An overview on studying 222 Rn exhalation rates using passive technique solid-state nuclear track detectors.* American Journal of Applied Sciences, 2012. **9**(10): p. 1653.

[36] Shafi ur, R., et al., *Determination of 238U contents in ore samples using CR-39-based radon dosimeter—disequilibrium case.* Radiation Measurements, 2006. **41**(4): p. 471-476.

[37] Barooah, D. and P.P. Gogoi, *Study of radium content, radon exhalation rates and radiation doses in solid samples in coal-mining areas of Assam and Nagaland using LR-115 (II) nuclear track detectors*. 2019, India: Vishal Publishing Company.

[38] El-Farrash, A.H., H.A. Yousef, and A.F. Hafez, *Activity concentrations of 238U and 232Th in some soil and fertilizer samples using passive and active techniques.* Radiation Measurements, 2012. **47**(8): p. 644-648.

[39] Abu-Jarad, F.A., *Application of nuclear track detectors for radon related measurements.* International Journal of Radiation Applications and Instrumentation. Part D. Nuclear Tracks and Radiation Measurements, 1988. **15**(1-4): p. 525-534.

[40] ICRP, *Human Respiratory Tract Model for Radiological Protection*, I.P. 66, Editor. 1994, ICRP.

[41] IAEA, *National and Regional Surveys of Radon Concentration in Dwellings*. 2014, Vienna: International Atomic Energy Agency.

[42] Rafique, M., et al., *Assessment of radiological hazards due to soil and building materials used in Mirpur Azad Kashmir; Pakistan.* 2011.

[43] Hogarth, D., *Classification and nomenclature of the pyrochlore group.* American Mineralogist, 1977. **62**(5-6): p. 403-410.

[44] Ringwood, A. and T. Irifune, *Nature of the 650–km seismic discontinuity: implications for mantle dynamics and differentiation.* Nature, 1988. **331**(6152): p. 131-136.

[45] Lumpkin, G.R., et al., *Retention of actinides in natural pyrochlores and zirconolites.* Radiochimca Acta, 1994. **66**(Supplement): p. 469-474.

[46] Lumpkin, G.T. and G.G. Dess, *Linking two dimensions of entrepreneurial orientation to firm performance: The moderating role of environment and industry life cycle.* Journal of business venturing, 2001. **16**(5): p. 429-451.

[47] Chitra, N., et al., *MODELING AND EXPERIMENTS TO ESTIMATE RADON EMANATION FACTOR IN SOIL—GRAIN SIZE AND MOISTURE EFFECT.* Radiation Protection Dosimetry, 2021. **194**(2-3): p. 104-112.

[48] ICRP, *Recommendations of the International Commission on Radiological Protection*, I. Publication, Editor. 1991, ICRP.

[49] Ayres da Silva, A.L.M., et al., *Radon in Brazilian underground mines.* J Radiol Prot, 2018. **38**(2): p. 607-620.

[50] Kumar, G., et al., *Radioactivity monitoring in the vicinity of Jawalamukhi thrust NW Himalaya, India for tectonic study*. Natural Hazards, 2022: p. 1-22.

[51] Yousef, H.A., et al., *Radon exhalation rate for phosphate rocks samples using alpha track detectors.* Journal of Radiation Research and Applied Sciences, 2016. **9**(1): p. 41-46.

[52] Mahur, A.K., et al., *Measurement of natural radioactivity and radon exhalation rate from rock samples of Jaduguda uranium mines and its radiological implications.* Nuclear Instruments and Methods in Physics Research Section B: Beam Interactions with Materials and Atoms, 2008. **266**(8): p. 1591-1597.

[53] Misdaq, M.A. and A. Mortassim, *222RN and 220RN concentrations measured in various natural honey samples by using nuclear track detectors and resulting radiation doses to the members of the rural populations in Morocco*. Radiat Prot Dosimetry, 2008. **130**(1): p. 115-8.

[54] Speelman, W.J., et al. *Radon generation and transport in and around a gold mine tailings dam in South Africa*. in *Second European IRPA congress on radiation protection - Radiation protection: from knowledge to action*. 2006. France.

[55] Yousef, H.A., et al., *Radon exhalation rate for phosphate rocks samples using alpha track detectors.* Journal of Radiation Research and Applied Sciences, 2016. **9**(1): p. 41-46.

[56] Shoeib, M. and K. Thabayneh, *Assessment of natural radiation exposure and radon exhalation rate in various samples of Egyptian building materials.* Journal of Radiation Research and Applied Sciences, 2014. **7**(2): p. 174-181.

[57] Yousef, H.A., et al., *Indoor radon concentration for phosphate rocks samples using CR-39 detector*. International Journal of Advanced Research in Science and Technology, 2015. **4**(3): p. 367-373.

[58] Kakati, R., *Radon exhalation rate of soil and indoor radon concentration of various places of Karbi Anglong District of Assam.* Journal of Applied physics, 2014. **6**(4): p. 13-16.

[59] Aswood, M.S., M.S. Jaafar, and S. Bauk, *Measuring Radon Concentration Levels in Fertilizers Using CR-39 Detector.* Advanced Materials Research, 2014. **925**: p. 610-613.

[60] Imtiaz, N. and M. Faheem, *Determination of 238U contents in ore samples using CR-39-based radon dosimeter—disequilibrium case.* Radiation Measurements, 2006. **41**(4): p. 471-476.